BBAA VI International Colloquium on:
Bluff Bodies Aerodynamics & Applications
Milano, Italy, July, 20-24 2008

CHARACTERISTICS OF ALONGWIND LOADS ON RECTANGULAR CYLINDERS IN TURBULENT BOUNDARY LAYER FLOWS

Chii-Ming Cheng[*], Ming-Shu Tsai[†], Jenmu Wang[#]

[*] Department of Civil Engineering, Tamkang University
151 Ying-chuan Road Tamsui,Taipei County Taiwan 25137
[*] e-mail: cmcheng@mail.tku.edu.tw, [†]austine@mail.tku.edu.tw, [#]wang@mail.ce.tku.edu.tw

Keywords: Alongwind load, Rectangular Cylinder, Wind Tunnel, Boundary Layer, Spatial Coherence.

1 INTRODUCTION

The alongwind loads of rectangular cylinders in turbulent boundary layers play important role in most building wind codes. This is an important topic which has been studied by many researchers through experimental or analytical methods. Most of the previous experimental investigations were based on high frequency force balance (HFFB) or limited number of pressure sensors. Although the global wind loads could be obtained through these procedures, details of the wind loads were lost due to the limitation of instrumentations. During past ten years or so, the high speed electronic pressure scanner system gradually becomes affordable and standard laboratory equipment. This high speed, multi-channel sampling capability makes the complete records of fluctuating wind pressure over the entire structural surface possible. Not only the conventional local wind pressure data or the global wind force characteristics can be obtained, the detailed load pattern and spatial correlations can also be acquired with little effort. This experimental procedure has been adopted by several researchers, Kareem [1], Lin et al. [2], to construct buildings aerodynamic database. This article presents partial results of the experimental works of a research project on the design wind loads of tall building. The semi-empirical model of the alongwind equivalent static design wind load was proposed in Cheng [3]. In which, several parameters such as local and global wind load coefficients on windward and leeward faces of the building, the longitudinal, lateral and span-wise spatial correlations are used. These parameters need to be obtained in turbulent boundary layers that can properly represent wind fields in urban, suburban and open country environments.

2 EXPERIMENT SETUP

To investigate wind loads on rectangular shaped tall buildings, pressure models were built and tested in a wind tunnel with test section of 17.0m (L) × 2.0m (W) × 1.5m (H). Three turbulent boundary layers, namely *BL-A*, *BL-B*, *BL-C*, with power law index α=0.32, 0.25, 0.15, respectively, were used to represent wind profiles over urban, suburban and open country terrains. The geometry variations of the pressure models are: aspect ratio $H/\sqrt{BD}$ = 3, 4, 5, 6, 7; side ratios D/B= 1/5, 1/4, 1/3, 1/2, 1/1, 2/1, 3/1, 4/1, 5/1. For model with aspect ratio of 7, 15

levels, 380 pressure taps were installed along the model height; and 9 levels, 230 pressure taps for pressure model with aspect ratio 3. The sampling rate was 200Hz and the sample length was 287 seconds. Besides the conventional mean and RMS base drag force coefficients C_D and C'_D, the windward and leeward drag coefficients, C_{Dw}, C_{Dl} and C'_{Dw}, C'_{Dl} are calculated, in which, $C_D = C_{Dw} + C_{Dl}$. All force coefficients are normalized with respect to model breadth, $q_H BH$. The reduced base drag spectra were normalized with respect to $(q_H BH^2)^2$. All testing cases were repeated to evaluate the error percentage of wind tunnel measurements.

3 RESULTS AND DISCUSSIONS

3.1 Effects of model geometry on wind loads

Shown in Figure 1 are the mean base drag coefficients of building with various aspect ratio and cross-sectional side ratio in open country flow field, *BL-C*. The windward face drag, C_{Dw}, increases with aspect ratio for all side ratio cases but remains almost invariant with respect to side ratio. For side ratio D/B<0.5, The drag on the leeward side, C_{Dl}, decreases slightly with increase of side ratio, then increases with side ratio afterwards. This side ratio effect can be attributed to the relative location of wake vortices to the leeward face and degree of reattachment. C_{Dl} decreases with increase of aspect ratio due to lower turbulence intensities for model with higher aspect ratio. As the result, the mean base drag coefficient, C_D, shows an opposite trend with C_{Dl}, i.e., for small side ratio models, when D/B<0.5, C_D increases slightly with increase of side ratio, then decreases with side ratio afterwards. Incident turbulence tends to weaken the wake structure and causes higher leeward pressure and lower drag, therefore, lower drag for lower aspect ratio.

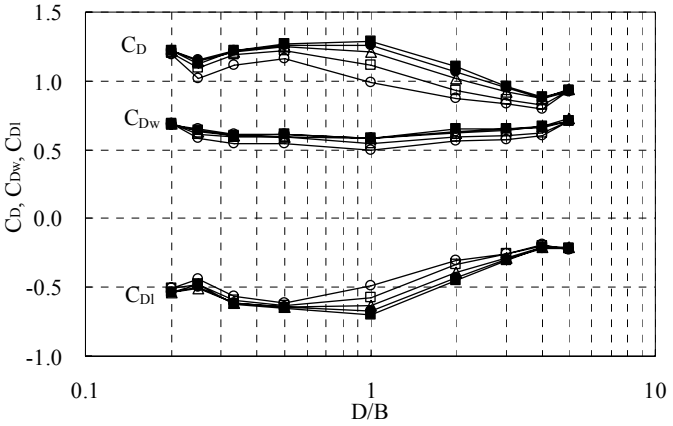

Fig.1 Variation of base drag force coefficients with side ratio in open country.
$H/\sqrt{BD}$ =○:3, □:4, △:5, ●:6, ■:7

The effect of side ratio on reduced drag spectra in open country flow field is shown

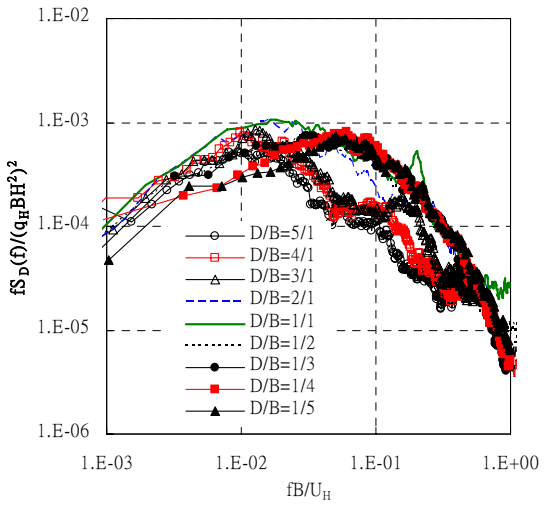

Fig.2 Variation of along-wind base moment spectra with side ratio ($H/\sqrt{BD} = 7$, Open country).

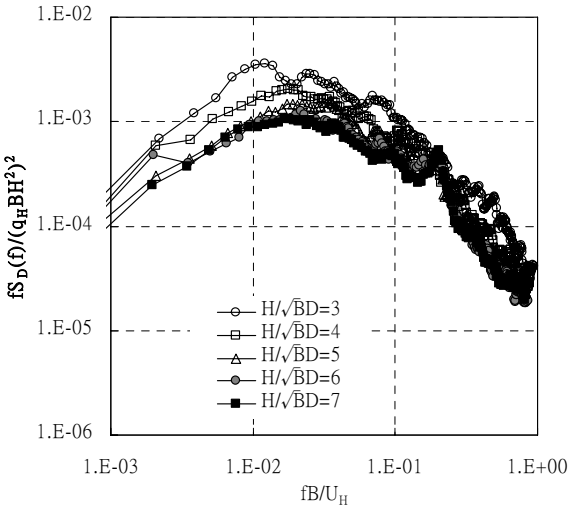

Fig.3 Variation of along-wind base moment spectra with aspect ratio (D/B=1, Open country).

in Figure 2. The drag spectra of various side ratios were clearly in two groups. For models with side ratio greater than 1.0, the drag spectra have significantly lower energy contents in the high frequency region and a secondary peak near fB/U_H=0.1~0.2, which is likely caused by the reattachment phenomenon. Similar result can be found in the case of urban and suburban flow fields. The drag spectrum of square shape, D/B=1.0, exhibits spectral peak at twice of the Strouhal frequency. Shown in Figure 3 are the reduced drag spectra of square shaped models with different aspect ratio in open country flow field. As the aspect ratio increasing, building model extended into higher elevation and lower turbulence intensity area, the spectral energy contents decrease noticeably, especially in the low frequency region. The drag spectrum of model with aspect ratio of 7 exhibits a clear spectral peak at twice of the Strouhal frequency.

3.2 Effects of boundary layer on wind loads

Shown in Figure 4 are the drag coefficients of building models in different boundary layer flows. The flow field condition does not have definite trend of influence on drag force for

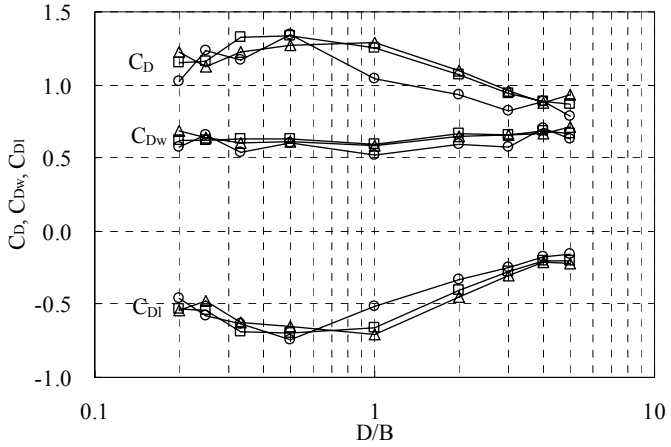

Fig.4 Variation of base drag force coefficients with side ratio and flow field condition ($H/\sqrt{BD}=7$).
○:Urban, □:Suburban, △:Open country

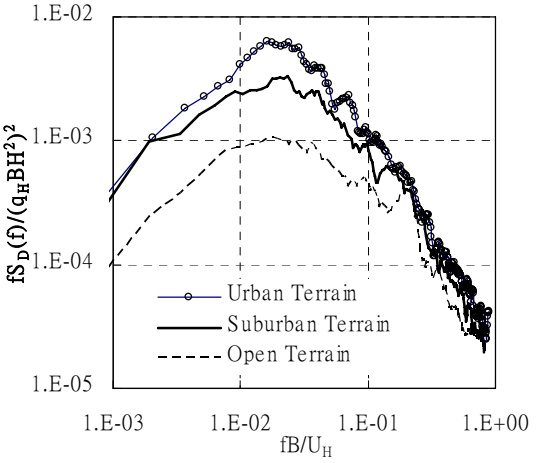

Fig.5 Variation of drag base moment spectra with flow field condition ($H/\sqrt{BD}=7$, D/B=1/1).

building with side ratio $D/B \leqq 0.5$. However, for $D/B \geqq 1.0$, urban flow field has the lowest absolute value of drag on both windward and leeward faces. Open country flow field exhibits slightly higher drag than suburban flow field. The most significant effect of flow field occurs at B/D=1.0. Shown in figure 5 are the reduced drag spectra of square shaped model with aspect ratio of 7 in different flow fields. There exists significant difference of spectral energy, especially in the energy contain region, among three different boundary layers. The fluctuating drag basically reflects the turbulence level of each flow field. A spectral peak at twice of the Strouhal frequency can be observed in the case of open terrain flow field; whereas it disappears completely in the urban terrain flow field.

3.3 Characteristics of spatial coherence of wind loads

Spatial coherences are important functions in the derivation of semi-empirical design wind load model. Shown in Figure 6(a)-6(c) are the coherence functions of the local wind loads on building model with aspect ratio of 6, side ratio of 1, in suburban flow field. In which, $R_z(\Delta z, f)$, $R_x(\Delta x, f)$ are the span-wise and lateral coherence functions, and $N(f)$ is the coherence between windward and leeward drag. Wind load coherences at 2/3 of model height, instead of

entire model, were used to represent $R_x(\Delta x, f)$ and $N(f)$ of the building. The wind tunnel measurements are then compared with the empirical exponential decay model proposed by Solari [4]. The exponential decay coefficients, C_N, C_x, C_z, are evaluated based on the current data.

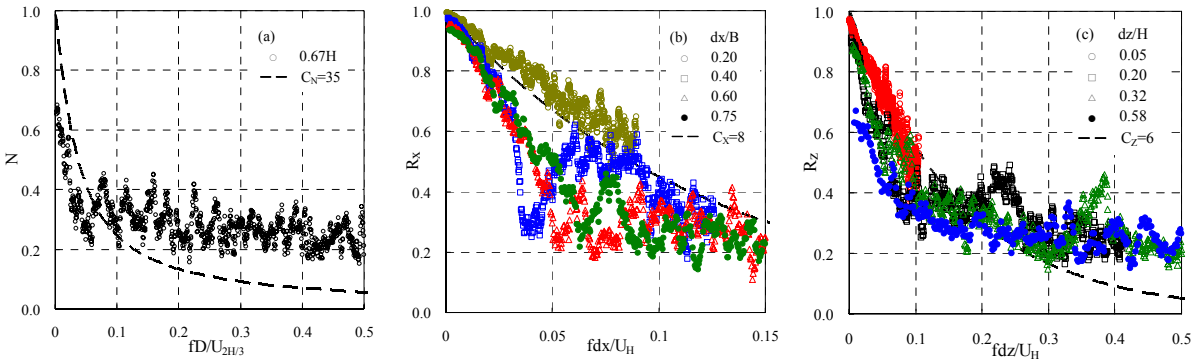

Fig.6 Coherence functions of local wind loads ($H/\sqrt{BD}=6$, $D/B=1$, Suburban).

Figure 6(a) indicates that $N(f)$ decreases rapidly initially and then remains nearly invariant. The lateral coherence $R_x(\Delta x, f)$, shown in Figure 6(b), has higher value in the case of small separation dx/B=0.2 and converges as dx/B increases. The span-wise coherence $R_z(\Delta z, f)$, shown in Figure 6(c), has slightly higher value at dz/H=0.05 and converges for the other dz/H. The dash lines are the fitted empirical exponential decay formulae of C_N=35, C_x =8 and C_z =6 which are determined primarily referenced to the data in lower reduced frequency region. Among them, C_x and C_z are small, whereas C_N is larger than the previously recommended [4]. Due to the page limitation, the spatial distribution of wind loads and statistical features such as peak factor and probabilistic parameters of drag force will be discussed in full paper.

4 CONCLUSIONS

A few remarks can be concluded based on this investigation: (1) For side ratio D/B<0.5, C_D increases slightly with increase of side ratio, then decreases with side ratio afterwards. Incident turbulence tends to weaken the wake structure and causes higher leeward pressure and lower drag for lower aspect ratio models. (2) Models of D/B>1.0 have significant lower energy contents in the high frequency region and a secondary peak due to reattach phenomenon. (3) The coherence decay coefficients, C_x and C_z are found to be smaller (higher correlation), whereas C_N is larger (less correlation) than previously recommended.

REFERENCES

[1] A. Kareem, (1997) “Correlation structure of random pressure fields.”, Journal of Wind Engineering and Industrial Aerodynamics 69-71, 507–516.

[2] N. Lin, C. Letchford, Y. Tamura, B. Liang, O. Nakamura, (2005), “Characteristics of wind forces acting on tall buildings.”, Journal of Wind Engineering and Industrial Aerodynamics 93, 217–242.

[3] C.M. Cheng, (2005), “Modifications on the alongwind design wind load”, The Fourth Africa-Europe Conference on Wind Engineering, Prague.

[4] G. Solari, (1987) “Turbulence modeling for gust loading.”, Journal of Structural Engineering, vol.113, no.7, 1550-1569.